Journal Pre-proofs

Super concentrated HCl in a deep eutectic solvent as media for the integrated leaching and separation of metals from end-of-life lithium-ion batteries

Ana R.F. Carreira, André Nogueira, Anna P.S. Crema, Helena Passos, Nicolas Schaeffer, João A.P. Coutinho

PII: S1385-8947(23)05105-7
DOI: https://doi.org/10.1016/j.cej.2023.146374
Reference: CEJ 146374

To appear in: *Chemical Engineering Journal*

Received Date: 23 June 2023
Revised Date: 31 August 2023
Accepted Date: 29 September 2023

Please cite this article as: A.R.F. Carreira, A. Nogueira, A.P.S. Crema, H. Passos, N. Schaeffer, J.A.P. Coutinho, Super concentrated HCl in a deep eutectic solvent as media for the integrated leaching and separation of metals from end-of-life lithium-ion batteries, *Chemical Engineering Journal* (2023), doi: https://doi.org/10.1016/j.cej.2023.146374

Super concentrated HCl in a deep eutectic solvent as media for the integrated leaching and separation of metals from end-of-life lithium-ion batteries

Ana R. F. Carreira, André Nogueira, Anna P. S. Crema, Helena Passos,* Nicolas Schaeffer,* João A. P. Coutinho

[a]CICECO - Aveiro Institute of Materials, Department of Chemistry, University of Aveiro, 3810-193 Aveiro, Portugal

*Corresponding authors. Email: nicolas.schaeffer@ua.pt; hpassos@ua.pt

Abstract

Recycling spent lithium-ion batteries is vital to ensure the recovery of added-value resources and minimize environmental impact. Herein, an integrated and efficient process is developed for metal recovery from spent cathode powder combining both leaching and transition metal separation in one step. A hydrophobic deep eutectic solvent (DES) is proposed as a HCl super concentrator for the one-pot leaching of cathodes from spent lithium-ion batteries and simultaneous Ni(II) precipitation. The DES composed of decanoic acid and trioctylphosphine oxide can super concentrate HCl, 2.2-folds more than the aqueous limit of 37 wt%, whilst being thermally and chemically stable under leaching conditions up to 373 K. The proposed leaching process can quantitatively extract Co(II), Mn(II) and Cu(II) from spent cathodes of laptop batteries whilst only extracting 10% of Ni(II). The latter could be easily recovered as $NiCl_2 \cdot 2H_2O$ with 99% purity through the manipulation of the coordination environment afforded by the DES relative to aqueous media. Key leaching parameters were the HCl:metal molar ratio and temperature, both having a significant impact on the leaching efficiency and its selectivity. Metal recovery was accomplished after stripping of the loaded DES solution *via* a straightforward sequential precipitation process, with 99% Co(II) and 98% Mn(II) being precipitated with 95% and 81% purity, respectively. The reported system presents a better atom economy compared to other DES and conventional inorganic acids, providing a new mild approach for the simultaneous leaching and separation of metals from lithium-ion batteries.

Keywords: spent cathode, HCl super concentrator, selectivity, metal recovery, atom efficiency.

1. Introduction

The world is transitioning towards cleaner and more sustainable energy sources. Renewable storage systems based on low-carbon technologies are increasingly relevant to address the intermittency of renewable energy sources and reduce fossil fuel dependency.[1,2] Lithium-ion batteries (LIBs) are widely used not only in energy storage technologies and electronic vehicles due to their high stability, low self-discharge rate, high energy density, high voltage and high capacity,[3,4] but also in most of small consumer electronics. This includes an estimated 7.2 billion globally active mobile phones and 1 billion laptop computers and tablets.[5] The widespread use of LIBs is forecasted to increase the demand for battery metals to 17.5 million tons (Mt) by 2030, representing more than a seven-fold increase between 2021 and 2030.[6] Battery metals include some raw materials classified as critical by the European Union, like cobalt and lithium, and also graphite, due to their supply risk issue and economic importance.[7] Consequently, LIB waste is estimated to surge from 0.6 Mt in 2020 to 2.0 Mt by 2023.[8] The embodied environmental footprint of consumer electronic manufacturing is heavily influenced by the extraction of its inherent metal content. Incorporating recycled materials in the manufacture of LIBs can lead to substantial reductions in energy consumption while affording superior rate and cycle performance.[9,10] Battery recycling in the EU is incentivized through legislation (Sustainable Batteries Regulation), which includes both specific targets for selected metals (cobalt, nickel, copper and lithium) and total recycling efficiency of 70 wt% by 2030.[11] As a result, there is a pressing demand for the development of LIB recycling processes.

Urban mining can decrease the environmental impact of end-of-life batteries while exploiting their inherent material value. End-of-life LIBs usually contain 5–20% cobalt, 5–10% nickel, 5–7% lithium, 5–10% other metals (primarily copper, aluminum, iron), 15% organic compounds (polymer, electrolyte, membrane), and 7% plastics.[12] However, the design of a robust and efficient recycling process is hampered by the lack of standard LIB cell design, multiple LIB chemistries (LCO, NMC, NMA, LFP), and the varying battery lifetime associated with the replacement rate of the final product (≈2 years for cell phones, ≈3–4 years for laptops and tablets and over 10 years for electric vehicles).[13,14] Managing end-of-life batteries can be accomplished *via* different methodologies such as pyrometallurgy, hydrometallurgy and direct physical recycling.[15–17] While direct recycling presents significant economic and environmental advantages, maintaining the cathode crystal structure requires meticulous sorting of cathode types and pre-treatment to avoid a final mixed product with an inferior value. Currently, no effective method is available for separating the cathode black mass, which refers to the active electrode materials after detachment from other components, based on its chemical composition.[18] Compared to pyrometallurgy, hydrometallurgy is a more promising alternative due to its lower energy requirements and gaseous emissions, as well as its greater process flexibility and ability to recover all metallic components from the black mass, including Li(I) and Mn(II).[19]

Hydrometallurgical treatment of LIBs occurs in three stages, namely leaching, individual metal separation, and final purification. The environmental impact of the final process is largely dependent on minimizing waste effluent quantities and toxicities, with life cycle assessments showing that the most significant environmental impact is caused by the leaching and wastewater treatment stages.[20–22] Conventional hydrometallurgical metal separation

presents environmental drawbacks due to the extensive use of concentrated inorganic acids and volatile organic solvents during solvent extraction.[23–25] Moreover, LIB leaching relies on the addition of reducing agents and generates large volumes of waste requiring neutralization.[25] A representative schematic example of a conventional hydrometallurgical process for LIB treatment is presented in **Figure 1**, showing the number of unit operations, many of which involve acid neutralization and careful pH control. Improvements are required to reach a greater atomic efficiency of each unit operation whilst ensuring their selectivity and substituting hazardous chemicals for more benign alternatives. Integrated processes capable of simultaneously combining multiple unit operations, such as leaching and separation, could provide additional economic and sustainability benefits by simplifying the overall flowsheet.

A potential approach to enhance the atomic efficiency of waste LIB processing is increasing the potency of a given acid by modifying its chemical environment.[26] It was previously shown that HCl could be "super concentrated" (increased molar ratio of HCl to water) relative to 37 wt% aqueous HCl under ambient conditions through its transfer from an aqueous to organic phase containing an amphiphilic extractant such as trioctylmethylammonium chloride (Aliquat 336), or trioctylphosphine oxide (TOPO).[27,28] Whilst acid super concentration is commonly observed in solvent extraction separations, few works harnessed its potential for metal leaching. Leveraging this potential offers several advantages, including reduced acid consumption, increased selectivity due to differing metal speciation between aqueous and organic media, and the suppression of hydroxide chemistry, thereby avoiding the formation of an inhibitory passivating layer during leaching.[29] Furthermore, apolar solvents with low water solubility can be easily regenerated by simply contacting the saturated phase post-leaching with an appropriate stripping solution, enabling the integration of the leaching and solvent extraction in a single stage. This strategy was previously employed for the preferential recovery of zinc and lead from iron-rich jarosite residues using HCl-equilibrated Aliquat 336, or for the selective leaching of palladium from platinum in a system of HCl and H_2O_2 in tributylphosphate (TBP).[30,31]

Such organic leaching systems must satisfy some criteria to ensure their applicability, namely:

- (i) a measurable improvement on aqueous leaching systems, either through improved selectivity and/or reduced acid consumption,
- (ii) present chemical and thermal stability under aggressive leaching conditions,
- (iii) be liquid at room temperature,
- (iv) have a moderate viscosity, and
- (v) the absence of phase splitting that can occur in organic systems at high metal or acid concentration.[32]

In this work, the hydrophobic deep eutectic solvent (DES) composed of TOPO:decanoic acid was identified as a promising HCl carrier for the leaching of LIBs. DES are low-melting binary mixtures of Lewis or Brønsted acids and bases with interesting properties due to the liquefaction and enhanced solubility provided by the decrease of the melting point of the mixture when compared to those of the starting pure constituents.[33] The reported HCl super concentration capacity of TOPO (melting point of 325.9 K) is harnessed through its incorporation as a DES constituent. The resulting liquid solution was acid-saturated and

subsequently optimized for the leaching of real end-of-life LIB cathode material. The choice of leaching media is based on the expectancy that the lower stability of the hydrated complex of Ni(II) chloride in the DES phase relative to the anionic chloro-complexes of competing transition metals ($[MCl_4]^{2-}$ where M= Cu, Co, Mn) will translate into minimal Ni(II) solubility, providing a simple approach to its direct separation.[34–36] A schematic representation of the proposed alternative metal leaching and recovery from spent cathode powder *versus* conventional approaches is depicted in **Figure 1**. Additionally, the use of DES removes the need for volatile organic diluents used in solvent extractions and avoids the critical problem of third-phase formation high metal loading.[28,34]

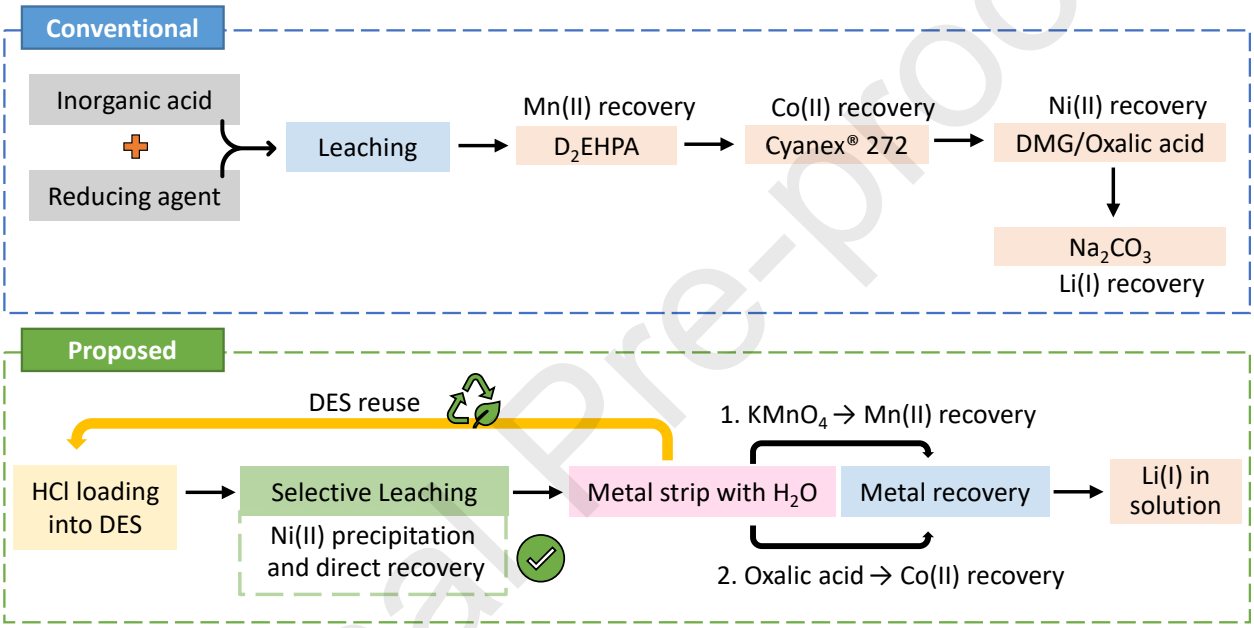

Figure 1. Schematic representation of spent cathodes leaching and metal recovery using conventional procedures and the proposed alternative DES leaching.[37,38] D_2EHPA and DMG stand for di-(2-ethylhexyl)phosphoric acid and dimethylglyoxime, respectively.

2. Experimental

2.1. Materials

Decanoic acid (> 98 wt%) was purchased from TCI. Hydrochloric acid (37 wt%) used throughout the work was purchased from Honeywell. Ammonia solution 25 v% was acquired from Labkem. Lithium chloride (99 wt%), magnesium sulfate·heptahydrate (> 99 wt%), nitric acid (65 wt%) and potassium permanganate (99 wt%) were purchased from Merck. Oxalic acid (98 wt%) was acquired from Alfa Aesar. Trioctylphosphine oxide (99 wt%), yttrium standard (1000 $mg \cdot L^{-1}$ of Y(III) in 2 wt% nitric acid), poly(vinyl alcohol) (> 99 wt%) and dimethyl carbonate (99 wt%) were acquired from Sigma Aldrich. Ethanol (analytical reagent grade) was purchased from

Fisher Scientific. Double distilled water was obtained through a Millipore filter system MilliQ® at room temperature. All chemicals were used as received.

2.2. Dismantling of end-of-life LIB and cathode separation

Laptop batteries from different brands were collected (**Table S1**). Each laptop battery contained around 4 to 6 LIBs. A multimeter was used to assess the voltage of each LIB. The spent LIB were discharged whenever necessary to ensure a safe dismantling (< 0.75 V). The LIBs were mechanically opened, followed by plastic shelling and electronic wires removal. The anode and cathode were manually separated. Electrolytes were removed by washing small sample portions with dimethyl carbonate (≈ 1 mL *per* g of cathode). The black mass (BM) containing the metals of interest was scrapped off from the aluminum foils by hand using a spatula. After washing the BM with water for 24 h at (313 ± 1) K, the sample was dried for 24 h at (323 ± 1) K before removal of the poly(vinylidene fluoride) binder by heat treatment in a furnace at 773 K for 2 h. The pre-treated BM was ground in a mortar to obtain a final homogenous powder used for all leaching experiments. The BM microstructure and morphology were evaluated by scanning electron microscopy with energy dispersive spectroscopy (SEM-EDS) in a HITACHI SU-70 apparatus operating at 25 kV after carbon sputter-coating powder X-ray diffraction (XRD) of the BM was carried out on a Bruker AXS with Cu Kα radiation operating at 45 kV and a 396 spinning discs sample holder. The obtained diffractograms were analyzed on the X'pert Highscore Plus software package.

2.3. Black mass leaching

Quantitative BM leaching was performed using *aqua regia* (50 v%) in a 44 $g \cdot L^{-1}$ solid:liquid ratio at (353 ± 1) K, 300 rpm for 6 h. The metal content on the leachate was quantified and deemed to represent complete leaching. The final BM residue was analyzed through XRD and SEM-EDS to further validate this.

Leaching optimization was carried out using the HCl-loaded DES as a leaching medium. Parameters such as the initial HCl concentration, solid:liquid ratio, temperature and time were evaluated. The DES composed of TOPO:decanoic acid was prepared gravimetrically (± 10^{-4} g) in a 1:1 molar ratio at (323 ± 1) K. After cooling, the DES was mixed with HCl in a 1:1 mass ratio for 1 h in an orbital shaker at 60 rpm and room temperature. The mixture was centrifuged for 10 min at 12 000 rpm, followed by phase separation. The chloride content in the HCl solution before and after DES contact was measured using a chloride ion-selective electrode (Metrohm). After contact with ranging HCl concentrations, the water content in the DES phase was determined on a Metrohm 831 Karl-Fischer coulometer with the analyte Hydranal-Coulomat AG from Riedel-de Haen. The HCl-loaded DES was then used to leach the BM at different conditions, followed by centrifugation for 10 min at 12 000 rpm. The metal content in the DES phase was quantified by total reflection X-ray fluorescence (TXRF).

The leaching extraction efficiency (*EE %*) was calculated as shown in **Equation 1**:

$$EE\ \% = \frac{[\mathrm{M}]_{\mathrm{extracted}}}{[\mathrm{M}]_{aqua\ regia}} \times 100\ \#1$$

where $[M]_{extracted}$ is the metal concentration in the DES (mol·kg^{-1}) and $[M]_{aqua\ regia}$ is the metal concentration in the *aqua regia* solution (mol·kg^{-1}). The separation factor (*Sf*) between two metals M_1 and M_2 was calculated according to **Equation 2**:

$$Sf_{M1/M2} = \frac{n_{M1}}{n_{M2}} 2$$

where n_{M1} are the moles of M_1 and n_{M2} are the moles of M_2 within the system.

2.4. Metal stripping and recovery

Metal stripping was accomplished by placing the metal-loaded DES in contact with water in a 1:1 mass ratio for 1 h at 60 rpm in an orbital shaker. The mixture was centrifuged for 10 min at 12 000 rpm and the metal content in the aqueous phase was determined. The stripping extraction efficiency was determined as described in **Equation 3**:

$$S\,\% = \frac{[M]_{stripped}}{[M]_{initial}} \times 100\ 3$$

where $[M]_{stripped}$ is the metal concentration stripped with water (mol·kg^{-1}) and $[M]_{initial}$ is the metal concentration that was initially in the DES (mol·kg^{-1}).

Metal recovery was accomplished through subsequential precipitation steps. Mn(II) was precipitated by adding $KMnO_4$ in a 1:1 molar ratio after adjusting the pH to 3.5 with ammonia 25 v%. Ultimately, Co(II) was precipitated at pH = 5.0 by adding a 1.2 molar excess of oxalic acid. The recovered precipitates were characterized by XRD.

2.5. DES reuse

The reusability of the DES was evaluated by performing five leaching-stripping cycles. After leaching, the mixture was centrifuged for 10 min at 3500 *g* and put in contact with water (1:1 m/m). The DES was then recontacted with HCl 8 mol·L^{-1} and the mixture was centrifuged for 10 min at 3500 *g*, followed by phase separation. The leaching and stripping extraction efficiency was evaluated throughout five cycles.

2.6. Metal quantification

The metal content (Co(II), Cu(II), Mn(II) and Ni(II)) in each leaching medium was quantified by TXRF using a Picofox S2 (Bruker Nano (Billerica, MA, USA)) with a molybdenum X-ray source. Quartz sample carriers were pretreated with 10 µL of silicon in an isopropanol solution and dried at (353 ± 1) K for at least 15 min. The samples were diluted in 1 g of a poly(vinyl alcohol) solution (1 wt%) and spiked with 10 µL of yttrium standard. Samples containing DES were diluted in a 1:1 mass ratio of an ethanol and poly(vinyl alcohol) solution. Ten microliters of each sample were added to the pretreated quartz carrier and dried on a hot plate at (353 ± 1) K for at least 30 min. Spectra acquisition time was set to 300 s. Unfortunately, although minor traces of aluminum are

anticipated in the BM, accurately quantifying this metal using TXRF was not possible due to the detection limit being greater than the concentration. For lighter elements, the intensity of the emitted X-rays is relatively weak and often falls below the detection limit of the TXRF system.

Lithium quantification was performed in an ion-selective electrode (Mettler Toledo Dx-series, USA). Ionic strength was buffered using $MgSO_4$. The calibration curve was prepared with LiCl concentrations ranging from 0.1 to 100 mmol·L^{-1}. Due to the hydrophobic nature of the eutectic solvent, lithium quantification was only feasible in the aqueous stripping solutions. After leaching, the UV spectra of the DES phase was evaluated using a SHIMADZU UV-1700 Pharma-Spec spectrometer.

2.7. Structural integrity and other properties

The structure of the pristine DES, DES loaded with HCl and DES after leaching was monitored by ^{1}H, ^{13}C and ^{31}P nuclear magnetic resonance spectroscopy (NMR) and Raman. Raman spectra were acquired on Bruker MultiRAM with a 1064 nm Nd-YAG laser source and a germanium detector cooled with nitrogen. Spectra were recorded ranging from 4000 to 100 cm^{-1} with a resolution of 4 cm^{-1}. The NMR spectra were recorded with 300.13 MHz or 75.47 MHz on a Bruker Avance III NMR spectrometer. Tetramethylsilane was added as an internal reference and $CDCl_3$ was used as a solvent.

The decomposition temperature (T_d) of the pristine DES was measured on a Setsys Evolution 1750 (SETARAM) instrument under a nitrogen atmosphere from 298 to 773 K with a heating rate of 5 K·min^{-1}. The stability of the DES at 377 K for 6 h under a nitrogen atmosphere was also evaluated.

Density (ρ) and dynamic viscosity (η) of the DES before and after leaching were measured at temperatures ranging from 293 to 353 K at atmospheric pressure in an automated Stabinger viscometer-densimeter (Anton Paar, model SVM3000). The temperature has a standard uncertainty of 0.02 K, dynamic viscosity has a relative uncertainty of 0.35% and density has an absolute uncertainty of 5×10^{-4} g·cm^{-3}.

3. Results and discussion

3.1. Black mass (BM) characterization

To ensure that the proposed approach is resilient towards the variability in LIB cathode chemistries, sixteen laptop battery packs (manufacturer and serial numbers listed in **Table S1**) were manually opened and sorted after safe battery discharge. The resulting BM was mixed and homogenized to yield a final representative composition, with this mixture being used in all subsequent leaching tests and optimizations. The resulting mixed BM was characterized by XRD (**Figure 2A**) and SEM-EDS (**Figure S1**), whilst the concentration of the leachable metal was quantified after *aqua regia* leaching (**Figure 2B**). The XRD analysis indicates the primary presence of $LiCoO_2$ (LCO) and $LiNi_xMn_yCo_zO_2$ (NMC) type chemistries in the BM. *Aqua regia* digestion of the BM, shown in **Figure 2B**, confirms cobalt as the most abundant transition metal with 0.04 mol·kg^{-1} of BM, followed by nickel (0.03 mol·kg^{-1} of BM) and manganese (0.005 mol·kg^{-1} of BM). Relative to the transition metals and considering the usual LIB cathode composition, a slight

stoichiometric excess of lithium was measured, most likely due to some residual content from the electrolyte. Although care was taken to separate the BM from the current collectors during manual disassembly, trace concentrations of copper were detected (0.001 mol·kg^{-1} of BM) in the final mixed waste. Similarly, minor traces of aluminum are expectable in the BM but its accurate quantification was not possible due to the concentration being below the equipment detection limit. The presence of elemental copper (and potentially aluminum) is liable to influence the final product's purity. However, it can positively contribute towards the leaching efficiency by acting as an effective reducing agent for LCO and NMC material.[39] The final solid fraction obtained after *aqua regia* leaching was analyzed by XRD and SEM-EDS (**Figure S2**), confirming the sole presence of carbon from the anode component in the residue. As such, the metal concentration obtained upon *aqua regia* leaching was considered representative of complete BM leaching and used to determine the extraction efficiency on the following leaching assays.

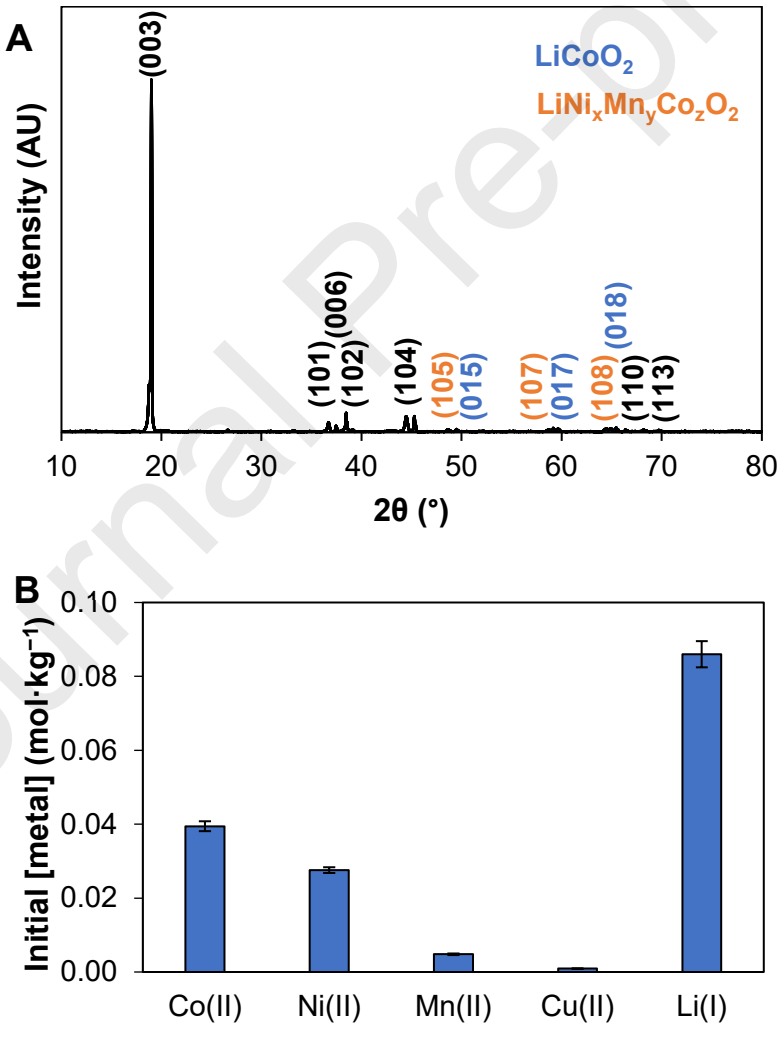

Figure 2. (A) XRD pattern of the BM from spent cathode materials. Orange labels refer to $LiCoO_2$ diffraction peaks, blue labels refer to $LiNi_xMn_yCo_zO_2$ and black labels are common to both LCO and NMC. (B) Leachable metal concentration in the BM quantified upon *aqua regia* leaching.

3.2. HCl loading and its effect on BM leaching

Whilst the affinity of TOPO for HCl was previously demonstrated when diluted in "inert" organic diluents, no such study exists upon its inclusion as a DES component. In a previous work using the TOPO:decanoic acid DES, the TOPO molar fraction (x_{TOPO}) was identified as the determinant factor dictating the final HCl concentration in the DES phase.[40] Nevertheless, as the solid-liquid phase diagram of the system imposes a practical restriction on the final DES liquidus composition at room temperature, a constant x_{TOPO} of 0.5 was used throughout as this offered the best compromise between maximizing HCl loading whilst minimizing unwanted crystallization.[34] Aqueous solutions of HCl with concentrations ranging from 4 to 12 $mol \cdot L^{-1}$ were placed in contact with the TOPO:decanoic acid mixture for 1 h at 1:1 mass ratio, an agitation of 60 rpm and at room temperature. After centrifugation and phase separation, the water and HCl concentrations in the DES phase were measured. The total concentration of HCl loaded into the DES phase and the corresponding evolution of the HCl to H_2O molar as a function of the initial aqueous HCl concentration are shown in **Figure 3A**.

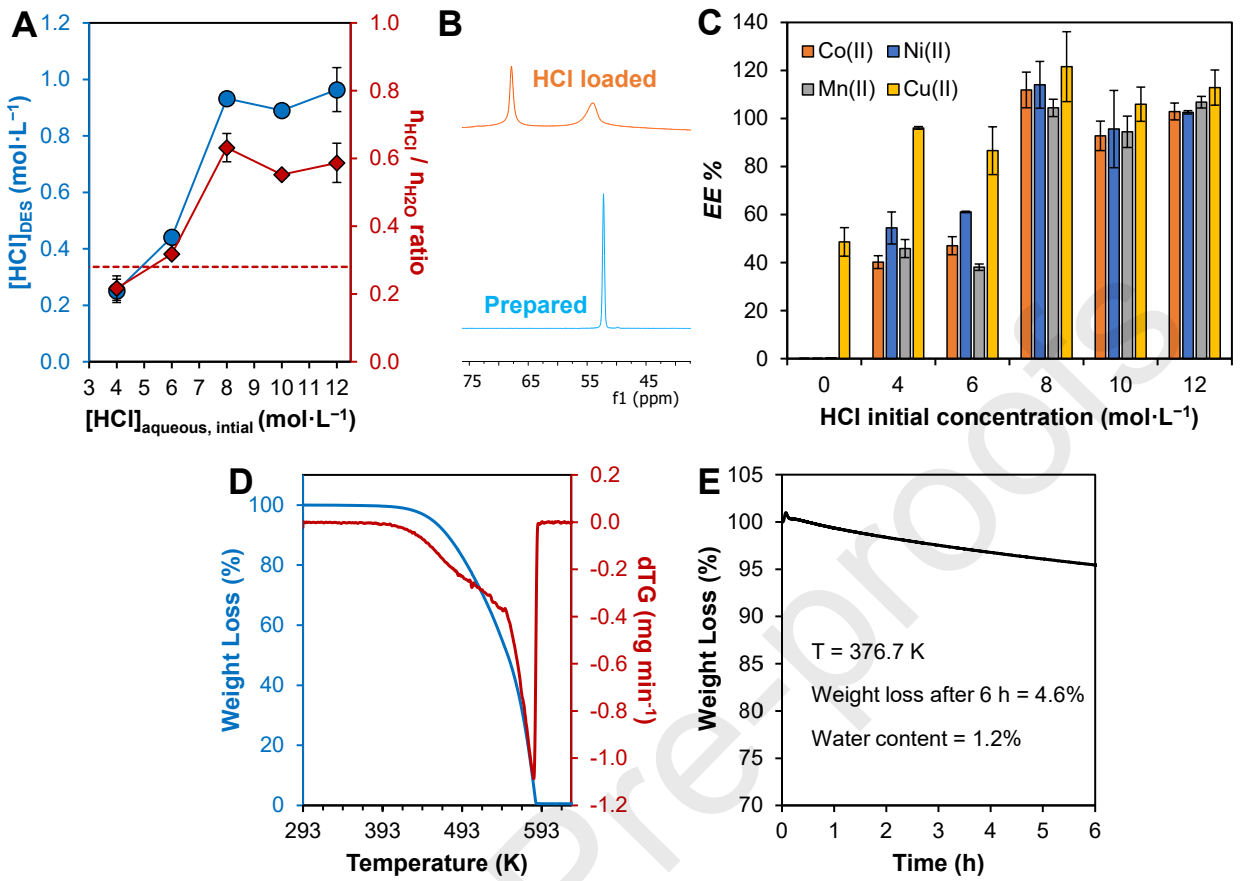

Figure 3. (A) Concentration of HCl (mol·L^{-1}) and molar ratio of HCl-to-H_2O in the loaded DES phase upon contact with different initial concentrations of HCl for 1 h at room temperature, 1:1 ratio (m/m) and 60 rpm. The dashed line represents the n_{HCl}/n_{H2O} of 37 wt% HCl. (B) ^{31}P NMR spectra of the DES before (blue line) and after (orange line) equilibration with an aqueous solution of 8 mol L^{-1} HCl. (C) Leaching extraction efficiency (*EE%*) at different initial aqueous HCl concentrations (mol·L^{-1}) at T = (373 ± 1) K, BM:DES ratio of 18 g·L^{-1}, 300 rpm and t = 6 h. (D) TGA of the pristine DES under N_2 atmosphere and a heating rate of 5 K·min^{-1}. (E) Isocratic TGA of the pristine DES at T = (377 ± 1) K for 6 h under N_2 atmosphere.

The loading of HCl into the DES phase improves as the initial HCl concentration increases up to 8 mol·L^{-1} after which a plateau is reached, achieving a maximum DES-phase concentration of (0.93 ± 0.02) mol·L^{-1}. While the conventional saturated HCl solution (37 wt%) displays a molar HCl-to-H_2O ratio (n_{HCl}/n_{H2O}) of 0.28, the DES phase can super concentrate HCl more than 2.3 times this value to 0.64. Loading HCl into the DES phase induces an acidic environment around the basic P=O group, causing a splitting of the original P=O band at 52 ppm and producing a down-field $\Delta\delta^{31}$P shift in the NMR spectra of the DES after HCl contact to 68 ppm, as shown in **Figure 3B**. This confirms the dominant role of TOPO in HCl extraction. However, when considering a TOPO concentration of 1.58 mol·L^{-1} in the prepared DES, the resulting molar fraction of TOPO to HCl is 0.61. Other solvent extraction experiments reported n_{TOPO}/n_{HCl} ratios greater than 1.5, indicating

a below than theoretical saturation capacity.[28,32] Moreover, far greater n_{HCl}/n_{H2O} values relative to aqueous solutions of 37 wt% HCl were obtained for TOPO (7.2) or Aliquat 336 (1.7) diluted in benzene.[28] The significant difference in n_{TOPO}/n_{HCl} and n_{HCl}/n_{H2O} between the TOPO incorporated as a DES component and diluted in benzene is attributed to the contrasting nature of intermolecular interactions in the two solvents. When diluted in an "inert" solvent such as benzene, TOPO has minimal interactions with the solvent molecules and can effectively extract HCl by forming reverse aggregates.[28,32] However, in the TOPO:decanoic acid mixture, intermolecular interactions lead to the formation of pre-organized phases with structural heterogeneity. The competing H-bonding interaction between TOPO:decanoic acid decreases the amount of "free" TOPO available for HCl extraction.[40,41] Previous small-angle X-ray scattering analysis (SAXS) analysis of the same eutectic system in the presence of HNO_3 suggested a homogeneous dispersion of the acid in the solvent.[41] A similar behaviour is expected in the studied HCl system. This is further supported by spectroscopic characterization of the DES phase before and after contact with HCl (**Figure S3**). Raman analysis confirmed both the chemical stability of the DES in the extended presence of HCl and the absence of the Cl_3^- peak, implying that HCl is most likely homogeneously distributed in the phase. Whilst TOPO is dominant in the superconcentration of HCl, the abundance of hydrogen bonds provided by decanoic acid is important (i) to ensure the liquefaction of the mixture under ambient conditions and (ii) to prevent phase splitting.[32,41] Third phase formation leads to the formation of a heavy and a light phase above certain HCl and metal concentration thresholds. This effect is undesirable as it restricts the solvent extraction operation at higher metal loading.

Incorporating HCl in the DES phase significantly enhances metal extraction from real BM, as shown in **Figure 3C**. The presence of HCl in the DES phase is required to successfully leach metals from the BM since only 48% of Cu(II) was extracted in its absence and no dissolution of the BM oxide component was observed. The leaching extraction efficiency increases until 8 $mol \cdot L^{-1}$ of HCl, being unaffected beyond this point, in accordance with the HCl loading results. When loaded with ≈ 1 $mol \cdot L^{-1}$ of HCl, the DES affords complete BM leaching considering a solid:liquid ratio of 18 $g \cdot L^{-1}$, a leaching time of 6 h, and a temperature of 373 K. These conditions were arbitrarily selected as screening conditions with a stoichiometric excess of HCl to BM and taking advantage of the greater boiling point of the DES relative to water. Unfortunately, the available analytical technique precluded the direct measurement of Li(I) in the DES phase although no trace of LiCl was detected in the residual solid phase. Detailed optimization of the leaching conditions is discussed further on. Additionally, as real waste BM matrix was used throughout, leaching results greater than 100% are expectable in some cases due to the small sample size used *per* assay and the waste heterogeneity. Based on the results in **Figure 3C**, all following leaching tests were carried out after equilibration of the DES phase with 8 $mol \cdot L^{-1}$ of HCl. Importantly from an energy consumption perspective, the heat capacity of the DES is estimated to be approximately half that of water (≈2.1 $J \cdot g^{-1} \cdot K^{-1}$ *vs* 4.182 $J \cdot g^{-1} \cdot K^{-1}$ for water), such that heating the DES to 373 K is energetically equivalent to commonly used aqueous leaching conditions of 323 K for a given time. The estimation is comparable to that reported for other DES, and it is based on the liquid phase heat capacity of decanoic acid (2.426 $J \cdot g^{-1} \cdot K^{-1}$) and the comparable triphenylphosphine oxide (1.804 $J \cdot g^{-1} \cdot K^{-1}$), assuming ideal mixing rule, in the absence of literature data for liquid TOPO.[42–44]

Beyond the ability to super concentrate HCl, which is accessible in a range of extractant-organic solvent mixtures, the eutectic system was identified as a promising carrier solvent for HCl due to its anticipated chemical and thermal stability. As such, a thermal study of the prepared eutectic mixture by TGA in N_2 atmosphere was performed under dynamic (**Figure 3D**; heating rate of 5 $K \cdot min^{-1}$) and static heating (**Figure 3E**). The DES was prepared under ambient conditions with no moisture control and had a water content of (1.19 ± 0.02) wt% measured by Karl-Fisher titration. The thermogravimetric profile of the pristine DES presents two distinct weight loss events, the first of these at 455 K attributed to the evaporation or degradation of decanoic acid followed by the rapid degradation of TOPO above 540 K. It is known that dynamic TGA analysis can lead to overestimations of thermal stability. To address this, static TGA was performed at 377 K, slightly above the screening leaching temperature shown in **Figure 3C.** After 6 h, a weight loss of 3.4 % was observed following the subtraction of the water content due to the slight volatility of the decanoic acid. This value was deemed satisfactory to proceed and to mitigate any potential losses, all subsequent leaching tests were performed in sealed vials.

3.3. Optimization of the BM:DES ratio and Ni removal

Contrary to initial expectations in which a degree of selectivity between the transition metals and Ni(II) was anticipated based on the differing ion speciation in the DES phase, leaching results in **Figure 3C** indicate a quantitative dissolution of all metal ions in the BM residue.[34,45] Assuming that the leaching of BM by HCl proceeds similarly in aqueous and DES media, the overall reaction is given by **Equation 4**:[46,47]

$$2\mathrm{LiMO}_{2,(s)} + 8\mathrm{HCl}_{(l)} \leftrightarrow 2\mathrm{LiCl}_{(l)} + 2\mathrm{MCl}_{2,(l)} + 4\mathrm{H_2O}_{(l)} + \mathrm{Cl}_{2,(g)} \#4$$

where M = Ni(II), Mn(II) or Co(II) and the subscripts indicate the solid, liquid, or gaseous phase. A limiting stoichiometric ratio of 1:4 BM to HCl is required to ensure the complete dissolution of all BM cations. At the studied solid-to-liquid concentration of 18 $g \cdot L^{-1}$ in **Figure 3C**, a molar excess of HCl is present in the DES phase (≈1:5 BM to HCl), which may explain the similar leaching efficiencies of Ni(II) to the other transition metals. As such, the BM-to-DES ratio was varied from 18 to 88 $g \cdot L^{-1}$ to evaluate its effect on the leaching efficiency for a fixed HCl loading of (0.93 ± 0.02) $mol \cdot L^{-1}$, with the results presented in **Figure 4A**.

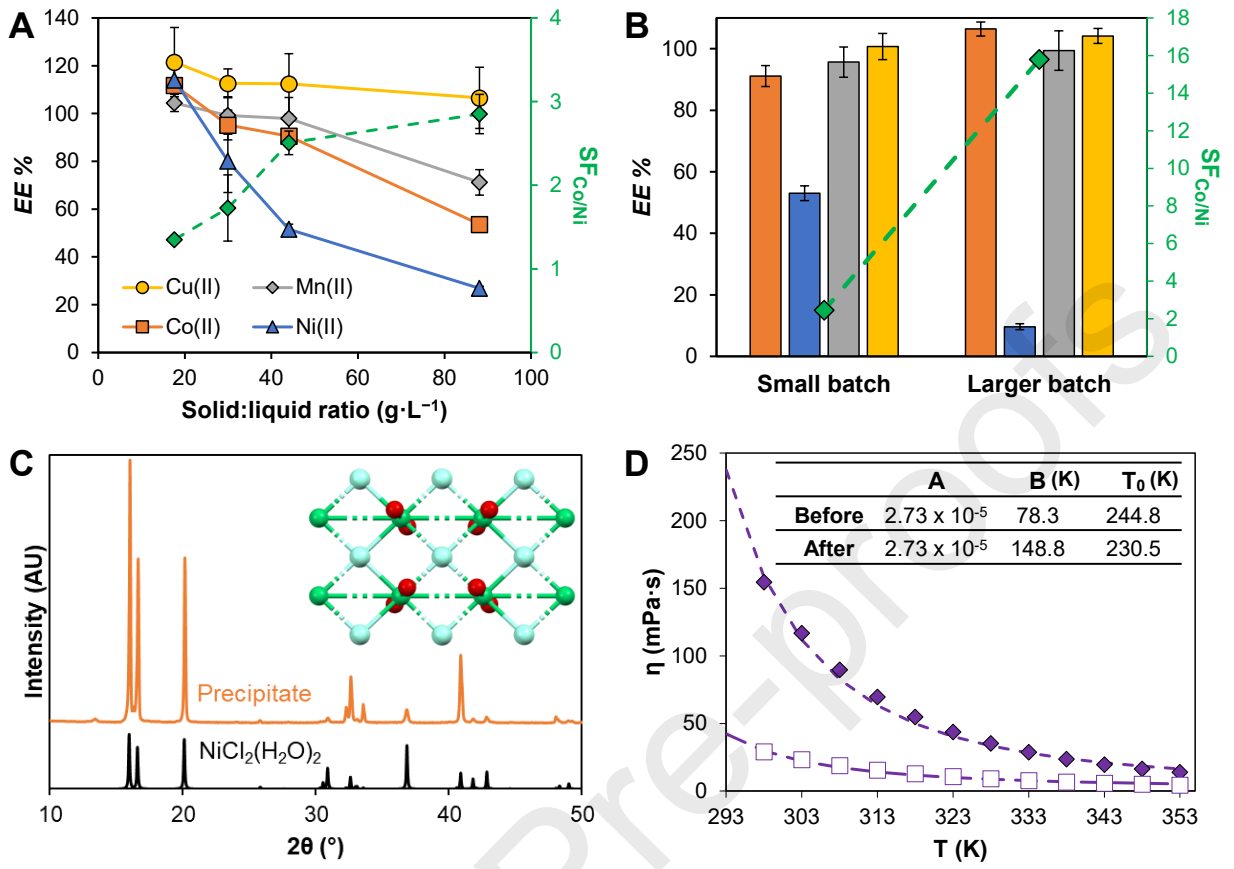

Figure 4. (A) Effect of the BM:DES solid to liquid ratio (g·L^{-1}) on the leaching efficiency (*EE%*) at T = (373 ± 1) K, 300 rpm for 6 h. The separation factor of Co(II) over Ni(II) ($Sf_{Co(II)/Ni(II)}$, green dashed line) is plotted in the secondary *Y*-axis. (B) Effect of scaling up on the leaching efficiency and Co(II)/Ni(II) separation (44 g·L^{-1} S/L, T = 373 K). (C) Powder XRD pattern of the precipitated residue during leaching (reference $NiCl_2{\cdot}2H_2O$ was predicted based on ICSD – 15351). Inset: $NiCl_2{\cdot}2H_2O$ unit cell with Cl atoms in green, Ni(II) in cyan and O in red (H not shown for clarity). (D) DES viscosity as a function of temperature before (empty symbol) and after (full symbol) BM leaching. The dashed lines represent the VFT fitting with the fitted parameters being provided in the table.

As expected, increasing the BM:DES ratio from 18 to 88 g·L^{-1} decreases the overall leaching efficiency except for Cu(II), which remains largely unaffected due to its presence in trace amounts. Importantly, a decorrelation in leaching efficiency between Ni(II) and the other transition metals is observed for a solid:liquid ratio between 30 and 44 g·L^{-1}, representing a BM to HCl molar ratio of 1:3.2 and 1:2.2, respectively. Under these conditions, the Ni(II) leaching efficiency was found to drop 52% whilst Mn(II) and Co(II) leaching remained above 95%, yielding a Co(II) to Ni(II) separation factor of 2.5 as *per* **Equation 2**. A BM-to-DES ratio of 44 g·L^{-1} was therefore selected for the following assays since it affords an adequate separation of Ni(II) while promoting close to full leaching of the remaining metals. Once dissolved, the stability of each metal in the more apolar DES phase depends on its ability to form stable chloro-

complexes.[35,45,48] The presence of the tetrahedral anionic chloro-complexes of the type $[MCl_4]^{2-}$ in the DES phase after leaching was further confirmed by UV–Vis analysis (**Figure S4**) in which the characteristic bands of $[CoCl_4]^{2-}$ are apparent between 550 to 750 nm as well as that of $[CuCl_4]^{2-}$ at 285 nm. For leaching conditions presenting deficient chloride concentrations, the competing chloride speciation between metal ions ensures a degree of selectivity, as is often exploited in solvent extraction to separate Co(II) from Ni(II) using basic extractants. Compared to the reported speciation of Cu(II) and Co(II), for which tetrahedral anionic chloro-complexes are accessible under ambient conditions, Ni(II) is unable to form fully dehydrated chloro-complexes.[35,49,50] Relative to aqueous HCl medium for which Ni(II) and Co(II) present comparable speciation below 2.0 mol L^{-1} HCl, the inclusion of dilute HCl in the lower dielectric DES phase permits to tailor the metal coordination environment as to achieve a selective leaching. A similar approach was reported in the hydrophilic DES composed of oxalic acid dihydrate and choline chloride diluted in DMSO, in which Ni(II) precipitated as nickel oxalate during leaching, leaving Co(II) and Mn(II) in solution as the anionic chloro-complexes $[MCl_4]^{2-}$.[51]

After separating the DES phase from the solid residue, a yellow-green precipitate would visibly form in the leachate over the following hours. To characterize the emerging solid phase and avoid cross-contamination due to the small leachate volumes used until then, the leaching reaction was scaled up from 0.5 g of DES to 12 g of DES, maintaining a fixed solid-liquid ratio of 44 g·L^{-1}. Importantly, the centrifugation conditions used after leaching in the small and larger batch differed due to the sample volume change. The centrifugation of the "larger" DES phase at 3500 *g* for 10 min fully separated the DES from the precipitate, with no further visible precipitate forming in the subsequent days. Analysis of the "larger" DES phase after removal of the precipitate, shown in **Figure 4B**, indicates a significantly lower Ni(II) extraction efficiency of (10 ± 1) % to yield an encouraging Co(II)/Ni(II) separation factor of 15.9, thereby permitting the simultaneous BM leaching and Ni(II) recovery in one step. The limited chloride availability at higher BM:DES ratios reduces the solubility of Ni(II) in the media, suggesting a dissolution-precipitation mechanism. Powder XRD of the recovered precipitates presented in **Figure 4C** indicates $NiCl_2{\cdot}2H_2O$ as the primary phase, whilst no Cu(II), Co(II), Mn(II), or Li(I) could be detected in the solid phase by TXRF or ion-selective electrode after redissolution in water, confirming its purity.

Scaling up the leaching reaction resulted in a significant Co(II)/Ni(II) selectivity improvement, which is intertwined with the notable change in the DES viscosity before and after leaching, as evidenced in **Figure 4D**. The experimental viscosity data were described with the Vogel-Fulcher-Tammann (VFT) equation (**Equation 5**):

$$\log_{10}\eta = A + \frac{B}{T - T_0} \quad 5$$

where A and B are fitting parameters and T_0 is the glass transition temperature. Fitted parameters are available in the inset of **Figure 4D**. Whilst a negligible viscosity difference was observed between the prepared and metal-laden DES for temperatures approaching the leaching conditions, a fivefold increase in the viscosity of the DES phase after leaching was recorded at 298 K, from 29.1 to 154.6 mPa·s.[51] Considering a complete dissolution of the BM for a solid-liquid ratio of 44 g·L^{-1}, this represents a metal ion (transition metal and Li(I)) to TOPO molar ratio of 3.92. The introduction of electrostatic interactions in a previously non-ionic system results in the emergence of ion-ion correlations arising from the $M^{+/2+}$ and Cl^- charge ordering as the

saturation limit of the DES is approached. This was previously observed experimentally by SAXS analysis in the same DES system loaded with 75 $g \cdot L^{-1}$ of $Eu(NO_3)_3$.[41] The increased viscosity poses a practical problem in separation and handling, requiring longer settling times and more vigorous centrifugation speeds to achieve a better Ni(II) recovery. This issue could be theoretically managed through the small addition of a high-boiling point co-solvent capable of also regulating the metal coordination environment.[51] However, this was not attempted herein due to the potential complications during Co(II) and Mn(II) recovery and solvent regeneration (*vide infra*).

3.4. Kinetic analysis and leaching comparison

To gain further insight into the leaching mechanism, the effect of temperature on metal leaching kinetics was evaluated using the DES loaded with 0.93 $mol \cdot L^{-1}$ HCl as a leaching media at a BM:DES ratio of 44 $g \cdot L^{-1}$. Due to its precipitation with time and the practical delay between sample leaching, centrifugation, and analysis, the leaching kinetics of Ni(II) was not assessed and was assumed to present a similar trend to Co(II) and Mn(II) before subsequently precipitating. Similarly, analytical limitations prevented the measurement of Li(I) directly in the DES phase, with only Co(II) and Mn(II) followed with time as well as the Cu(II) impurity. The dissolution kinetics at 333 K, 353 K, and 373 K are presented in **Figure 5A to 5C,** respectively.

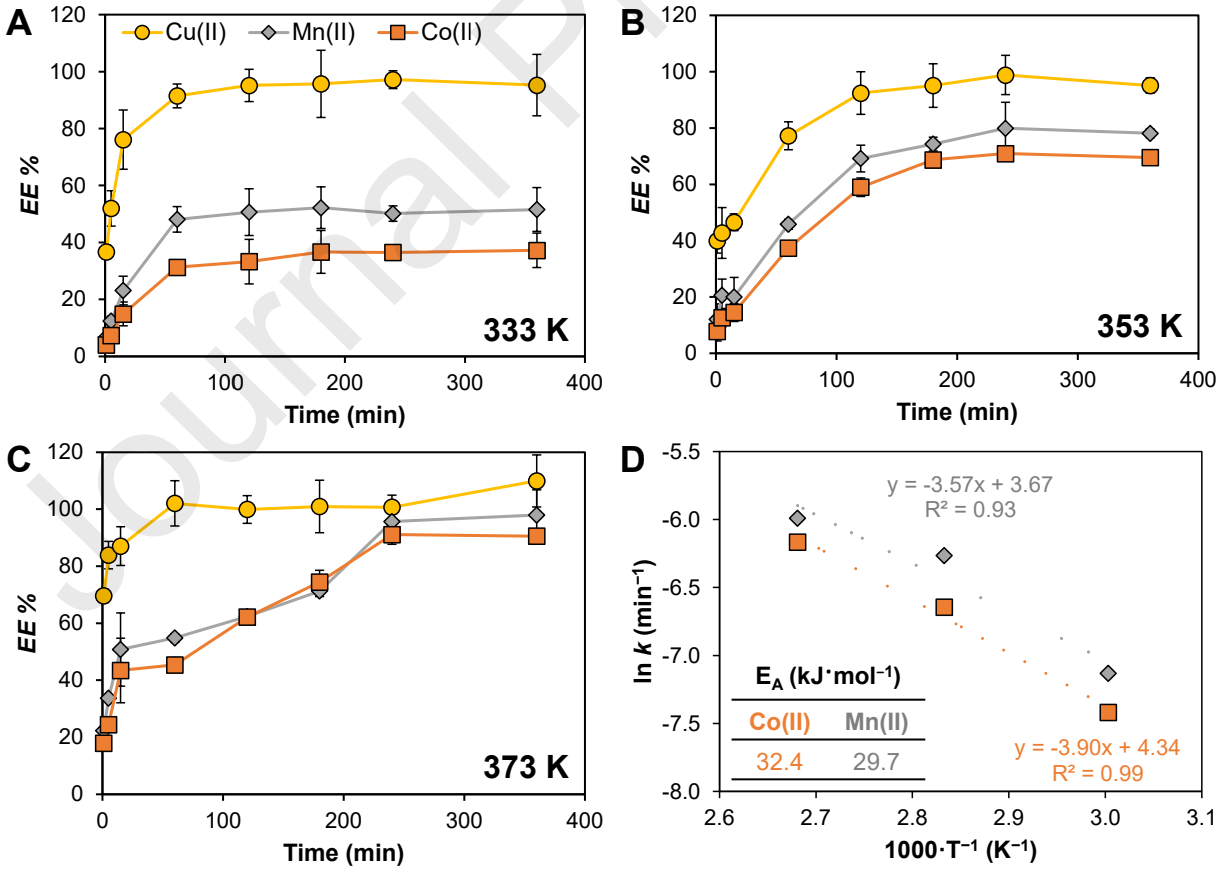

Figure 5. Temperature effect at (A) 333 K, (B) 353 K and (C) 373 K (± 1 K) on the metals leaching extraction efficiency (*EE %*) at 300 rpm and up to 360 min. (D) Arrhenius plot for the leaching of Co(II) and Mn(II).

Overall, the extraction efficiency improves as the temperature increases from 333 to 373 K but the maximum extraction efficiency at each temperature is attained faster at lower temperatures: 60 min at 333 K, 180 min at 353 K and 240 min at 373 K. The best extraction efficiency was obtained after 240 min of leaching at 373 K with (101 ± 4) % Cu(II), (91 ± 3) % Co(II) and (96 ± 5) % Mn(II) extracted. Several kinetic fittings were attempted on the experimental kinetic data to understand the underlying mechanisms. The rate-controlling step within the system was investigated based on the following shrinking core models (SCM) assuming spherical particles:

$$1-(1-x)^{\frac{1}{3}}=kt \quad 6$$

$$1-3(1-x)^{\frac{2}{3}}+2(1-x)=kt \quad 7$$

$$\left[(1-x)^{-\frac{1}{3}}-1\right]+\left(\frac{1}{3}\right)\ln(1-x)=kt \quad 8$$

where *x* is the fraction reacted in time *t* (min) and *k* (min^{-1}) is the specific rate constant of each model. **Equation 6** refers to the surface chemical control model, **Equation 7** corresponds to the diffusion control model and **Equation 8** is a mixed-controlled process involving a combination of film diffusion and chemical reaction. Among the tested fittings, the best correlation plots for Co(II) and Mn(II) were achieved with the diffusion control model (**Table S2**). However, the fitting of Cu(II) was inadequate despite the adjusted model and was not considered in the following discussion. This is most likely due to its presence in trace concentrations as well as the heterogeneity of the real waste matrix used. The reaction rate constant assuming a diffusion-controlled process (**Equation 7**) was used, along with the corresponding temperatures, to determine the apparent activation energies (E_a) of Co(II) and Mn(II) leaching according to the Arrhenius equation (**Equation 9**), with the Arrhenius plots presented in **Figure 5D**.

$$\ln k=\ln A-\frac{E_a}{RT} \quad \#9$$

where A is the frequency factor, E_a is the apparent activation energy ($J\cdot mol^{-1}$), R is the gas constant ($J\cdot mol^{-1}\cdot K^{-1}$) and T is the temperature (K). The plot of ln*k* vs $1000\cdot T^{-1}$ (**Figure 5D**) enables calculating the activation energy of the leaching reaction of each metal. From the resulting slope, a leaching activation energy of 32.4 and 29.7 $kJ\cdot mol^{-1}$ was obtained for Co(II) and Mn(II), respectively. Activation energies in the order of 20 $kJ\cdot mol^{-1}$ are typically assigned to diffusion-controlled leaching, whereas values greater than 40 $kJ\cdot mol^{-1}$ are attributed to chemical reaction-controlled leaching.[52] The lower activation energies of Co(II) and Mn(II) dissolution indicate

that this process is primarily diffusion-controlled. However, a mixed diffusion-reaction process cannot be excluded considering the need for metal reduction of the oxidized BM during leaching. The obtained activation energies are inferior to those reported for transition metal leaching using HCl, in the range of approximately 80 to 100 $kJ \cdot mol^{-1}$ depending on the BM chemistry, but comparable to E_a values for reductive leaching conditions (acid + reducing agent).[53]

Based on the leaching results, optimized conditions of T= 373 K, t = 240 min and a S/L ratio of 44 $g \cdot L^{-1}$ were identified for a DES phase pre-equilibrated with an 8 $mol \cdot L^{-1}$ HCl aqueous solution. An important aspect not addressed is the requirement for a reducing agent, as this is known to facilitate BM dissolution whilst reducing acid consumption. The reduction potentials of the active materials and potential reducing agents in the leachate are given in **Table 1**.

Table 1. Reduction potentials at 303 K of the primary BM active materials and potential reducing agents.

Half-cell reaction	E^0 *vs* SHE	Ref.
$Co^{3+} + e^- \rightarrow Co^{2+}$	1.97	[54]
$MnO_2 + 2e^- + 4H^+ \rightarrow Mn^{2+} + 2H_2O$	1.22	[55]
$Cl_2 + 2e^- \rightarrow 2Cl^-$	1.36	[56]
$Cu^{2+} + 2e^- \rightarrow Cu$	0.33	[54]
$O_2 + 4H^+ + 4e^- \rightarrow 2H_2O$	1.23	[56]
$O_2 + 2H^+ + 2e^- \rightarrow H_2O_2$	0.69	[54]

Considering a two-electron reduction process, the concentration of Cu(II) is insufficient to fully reduce the oxidized oxide content of the BM. In the absence of an additional reducing agent, it is probable that species typically considered oxidants, such as dissolved oxygen, water, and emitted chlorine during the leaching reaction, act as reducing agents for Co(III) and Mn(IV) in the studied system to facilitate the reductive leaching of the higher valence oxides. The careful management of the generated Cl_2 is crucial to ensure safety and prevent any harmful effects. Industrially, the scrubbing of chlorine gas is typically achieved by passing the collected gas generated during leaching through an alkaline solution of NaOH to generate sodium hypochlorite (NaOCl) and NaCl. The obtained results in DES are compared against reported leaching efficiencies using inorganic acids in the presence of reducing agents, with the results compiled in **Table 2**. As most reports do not have comparable leaching conditions to those used in the DES, two leaching assays were also conducted using 1 $mol \cdot L^{-1}$ HCl at 373 K for 120 and 240 min in aqueous solutions under reflux for a fairer comparison.

Table 2. BM leaching conditions and respective metal extraction efficiencies reported in the literature.

Leaching reactants	T (K)	Time (min)	S/L ratio ($g \cdot L^{-1}$)	*EE*%	Ref.
1 $mol \cdot L^{-1}$ H_2SO_4	368	240	50	93% Li, 66% Co, 96% Ni, 50% Mn	[57]
1 $mol \cdot L^{-1}$ H_2SO_4 + 0.075 $mol \cdot L^{-1}$ $NaHSO_3$	368	240	20	96% Li, 92% Co, 96% Ni, 88% Mn	[58]
3.5 $mol \cdot L^{-1}$ HCl + 4 $mol \cdot L^{-1}$ NH_4Cl + H_2O_2	353	180	125	100% Li, 100% Co 100% Ni, 100% Mn	[53]
1 $mol \cdot L^{-1}$ HNO_3 + 1.7 v% H_2O_2	348	30	20	95% Li, 95% Co	[59]
4 $mol \cdot L^{-1}$ NH_3 + 1.5 $mol \cdot L^{-1}$ $(NH_4)_2SO_4$ + 0.5 $mol \cdot L^{-1}$ Na_2SO_3	353	300	10	95% Li, 81% Co, 90% Ni, 4% Mn	[60]
2 $mol \cdot L^{-1}$ citric acid + 1.25 v% H_2O_2	333	120	30	81% Li, 93% Co	[61]
4 $mol \cdot L^{-1}$ HCl	353	120	–	97% Li, 99% Co	[62]
4 $mol \cdot L^{-1}$ HCl	363	1080	0.05	100% Li, 100% Co, 100% Ni, 100% Al	[63]
1.75 $mol \cdot L^{-1}$ HCl	323	90	0.2	99% Li, 99% Co, 99% Mn	[64]
1 $mol \cdot L^{-1}$ HCl	373	120	44	71% Li, 43% Co, 91% Ni, 72% Mn, 102% Cu	This work
1 $mol \cdot L^{-1}$ HCl	373	240	44	98% Li, 48% Co, 89% Ni, 82% Mn, 102% Cu	This work
0.93 $mol \cdot L^{-1}$ HCl in DES	373	240	44	106% Co, 10% Ni, 99% Mn, 104% Cu	This work

Overall, leaching with the DES mixture yields similar or better results than reported conventional leaching media while avoiding the need for reducing agents and providing a greater selectivity for Co(II) relative to Ni(II). Leaching with 1 $mol \cdot L^{-1}$ aqueous HCl under the same conditions affords lower extraction efficiencies than the DES-loaded with a comparable HCl concentration. The DES plays a key role in the leaching selectivity. Whereas the aqueous HCl leaching at 120 and 240 min have a $Sf_{Co(II)/Ni(II)}$ of 0.7 and 0.8, respectively, the DES-loaded with HCl affords a $Sf_{Co(II)/Ni(II)}$ = 15.9 at the same conditions. Herein, both HCl and DES are essential for achieving good extraction efficiencies while maintaining a promising Co(II)/Ni(II) selectivity. As a further measure of comparison, the atom economy (AE %) of the proposed leaching was calculated according to **Equation 10**:

$$AE\ \% = \frac{React_{used}}{React_t} \times 100 \quad 10$$

where $React_{used}$ is the stoichiometric mass of the used reactant and $React_t$ is the stoichiometric mass of the total reactant in the system. Herein, the DES is used as a selective scaffold while HCl is the reactant, as shown by the lack of transition metal leaching in the absence of HCl in **Figure 3C**. Under optimal conditions, all metals are leached with 0.93 $mol \cdot L^{-1}$ of HCl, affording a leaching atomic economy of (94.9 ± 5.7) %. This value is likely a slight overestimation as it does not

consider the reducing contribution of water and copper under the extraction conditions, positively contributing to the BM leaching and lowering the consumption of HCl. The atom economy was conservatively assumed as 89% (lower bound estimate) and further compared with that of other reported leaching reactions (**Figure 6** and **Table S3**) using hydrophilic DES based on organic acids, hydrophobic DES, and aqueous inorganic acid leachates. Similarly, the atom efficiency of the inorganic acids is likely overestimated as they rely on reducing agents, whilst choline is known to also act as a reducing agent during BM dissolution.[65] The developed leaching system affords a better atom efficiency than conventional leaching media and other DES, including the hydrophobic DES composed of TOPO:benzoyltrifluoroacetone (HBTA). By using the DES to stabilize the leached metal ions through complexation and HCl as a reactant, it is possible to develop a selective, efficient, and greener process in line with the principles of green chemistry.

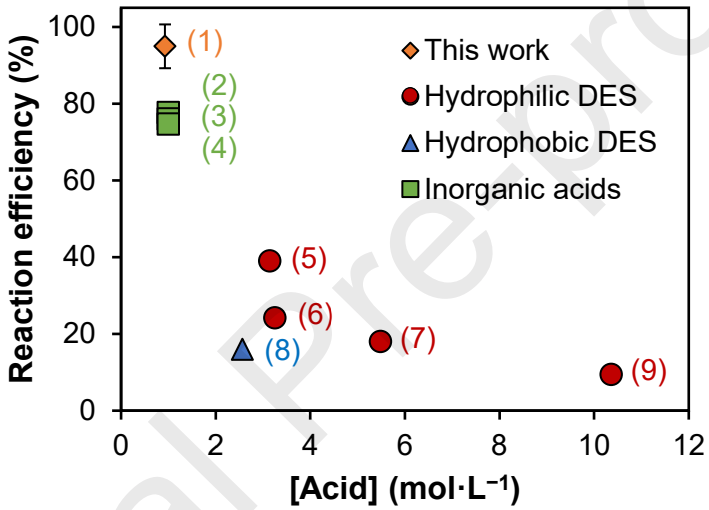

Figure 6. Atom efficiency of reported leaching media for spent cathodes, including for (1) our DES + HCl leaching results, (2) HNO_3 + 1.7 v% H_2O_2, (3) H_2SO_4 + 0.075 mol·L^{-1} $NaHSO_3$, (4) HCl (this work), (5) ChCl:TosA:H_2O (1:1:2), (6) ChCl:LacA (2:1), (7) ChCl:OxA (1:1), (8) HBTA:TOPO (2:1), (9) ChCl:ForA (1:2). The atom efficiency of the DES was calculated based on their respective acid concentration and assuming a leaching stoichiometry of 4:1 acid to LCO or NMC molar ratio.[59,60,66–70] The leaching conditions used to estimate the reaction efficiency are available in **Table S3**. (ChCl – Choline chloride; ForA – formic acid; OxA – oxalic acid; LacA – lactic acid; TosA – p-toluenesulfonic acid; HBTA – benzoyltrifluoroacetone).

3.5. Metal recovery and DES reuse

Following leaching, the DES phase could be easily regenerated by placing it in contact with water in a 1:1 mass ratio for 1 h at 60 rpm and room temperature. The mass ratio of the DES to water during stripping was not optimized, it is possible that complete stripping could be achieved

using a smaller water volume. This ratio was selected for practicality to minimize any potential cross contamination between phases during their separation for recycling and reuse. The presence of added water breaks the chloro-complexes present in the DES phase, allowing for the simple stripping of the extracted metals. This can be visually followed by the change from a blue/green coloration of the DES phase characteristic of $[CoCl_4]^{2-}$ to its migration to the aqueous phase resulting in the red coloration of $[Co(H_2O)_6]^{2+}$ as shown in **Figure S5**. Density plays a vital role in the DES-water demixing as phases must comprise a density difference of approximately 0.10 or greater to allow quick separation under settling conditions. The density difference between water and the metal-laden DES at room temperature is 0.08, promoting a relatively rapid demixing which was accelerated by centrifugation (**Figure S6**).

After centrifugation and phase isolation, a metal-rich aqueous phase and the DES with metal traces were recovered. Metal recovery from the aqueous strip solution (initial pH = 1.2) was accomplished *via* a sequential two-step precipitation. First, $KMnO_4$ was added to the metal-rich aqueous solution at pH 2.5 in a 1:1 molar ratio relative to the dissolved Mn(II) concentration, causing the formation of a dark brown precipitate. Oxidative precipitation by potassium permanganate is a widely utilized process for manganese removal based on the redox potential of the MnO_4^-/Mn^{2+} of E^0=1.51 V as indicated by the Pourbaix diagram of manganese.[55] The recovered precipitate was washed with water, calcinated at 823 K for 8 h and analyzed by XRD (**Figure 7A**), confirming the sole presence of the crystalline phase Mn_3O_4. The precipitation yield was determined by mass balance as 98% with a final commercial grade purity of 81%, Cu(II) being the major co-impurity representing 8% of the precipitate metal content. Secondly, the now cobalt-rich aqueous solution pH was adjusted to 5.0 and oxalic acid was added in a 1.2 molar excess relative to Co(II). A light pink precipitate was formed and characterized by XRD after drying at 323 K (**Figure 7B**), indicating the presence of cobalt oxalate dihydrate. The precipitation yield of Co(II) was 99%, with a final purity of 95%, as residual Ni(II) and Cu(II) present in the solution were also precipitated in this step. Consequently, Li(I) was the only component remaining in the aqueous solution. From this simple approach, a full process including mass balance of each metal is summarized in **Figure 7C**.

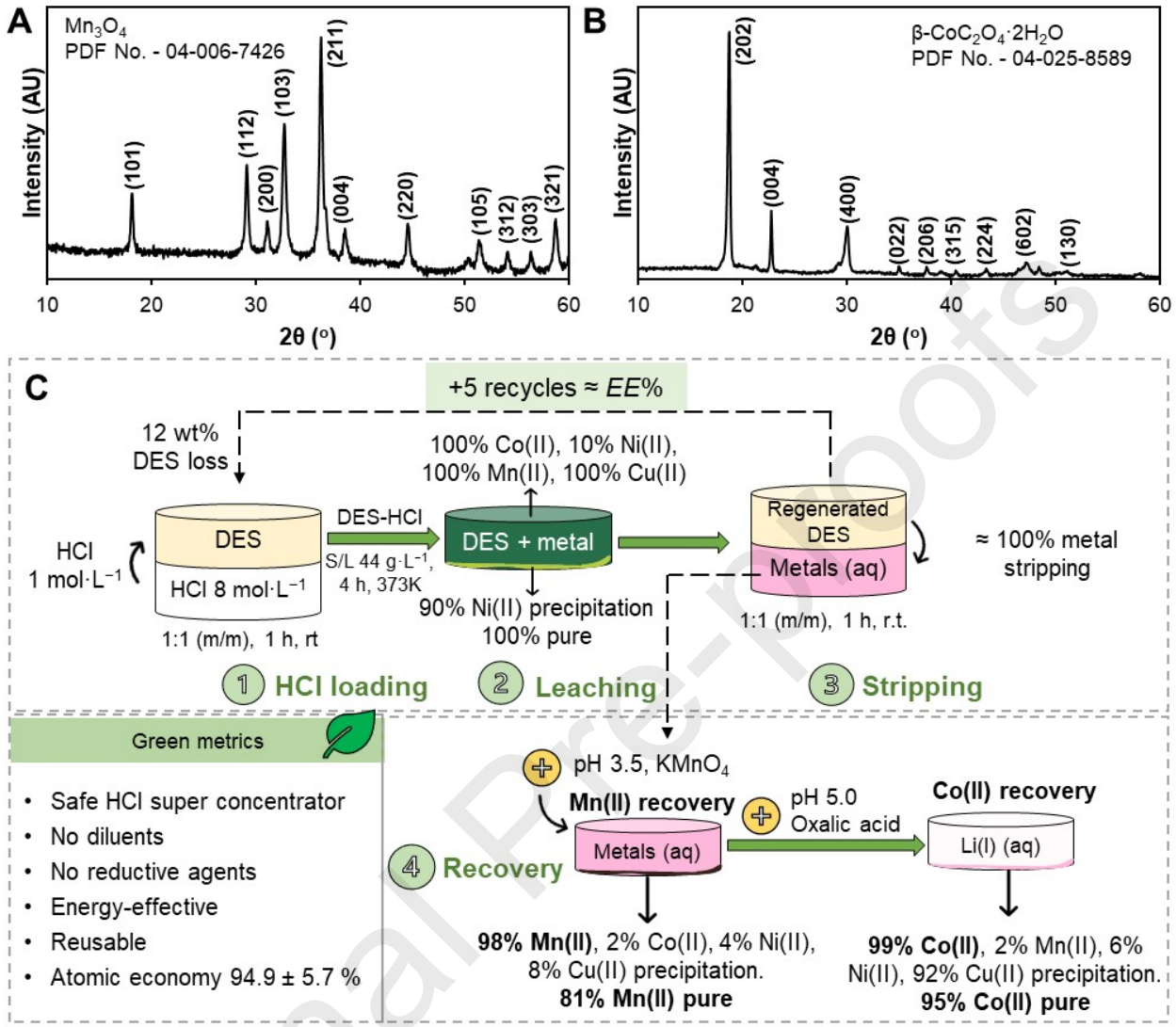

Figure 7. Powder XRD of the recovered product after addition of (A) a stoichiometric amount of $KMnO_4$ relative to the dissolved Mn(II) concentration and (B) 1.2x stoichiometric amount of oxalic acid relative to the dissolved Co(II) concentration. (C) Process diagram of the selective leaching and recovery of strategic metals from BM using TOPO:decanoic acid loaded with 0.93 mol·L^{-1} of HCl, including the DES phase regeneration and reuse.

Finally, the ability to reuse the DES in several consecutive leaching assays was evaluated to maximize the benefits of the proposed approach. As HCl is almost fully consumed during the leaching reaction, it is necessary to reintroduce the inorganic acid into the DES phase in-between leaching cycles. After each leaching cycle, the DES phase was stripped and regenerated with water prior to recontacting with an aqueous 8 mol·L^{-1} HCl solution to load 0.93 mol·L^{-1} of HCl in the DES phase. The extraction and stripping efficiencies throughout the five cycles are represented in **Figure 8**. The extraction of Co(II), Mn(II) and Cu(II) remained constant at ≈ 100%

for five leaching cycles. Importantly, the selectivity of the system for the Co(II)/Ni(II) pair stayed approximately constant and reaching as high as 79 during the 4th cycle, most likely due to the variability of the waste matrix. The stripping efficiency was also stable and close to quantitative over five stripping cycles, with Li(I) being the only exception. Since the TOPO:decanoic acid mixture is not water-miscible, it is not possible to quantify Li(I) on the leaching samples using our available analytical techniques. For this reason, it is unclear if the leaching reaction of Li(I) was incomplete or if the Li(I) stripping was not entirely successful as TOPO-based DES were shown to be effective Li(I) extraction media[71]. Despite this, the DES showed a great regeneration capacity without losing efficiency or selectivity even after five consecutive leaching-stripping cycles. Unfortunately, in between cycles approximately 12 wt% of DES was lost due to the difficulty in handling small sample size and the increased viscosity after leaching. This could be foreseeably mitigated using larger batch sizes as well as increasing the centrifugation temperature.

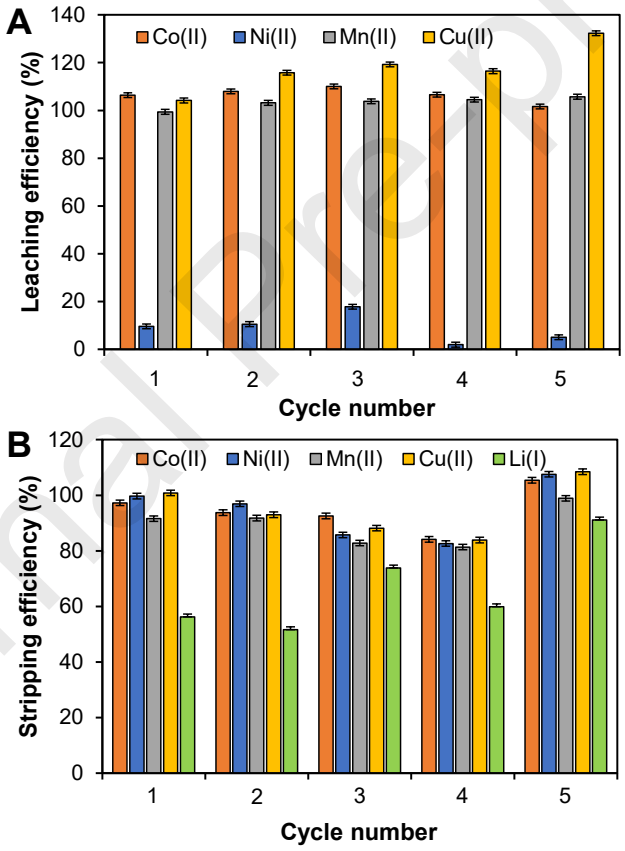

Figure 8. (A) Extraction efficiency across the different leaching cycles at 44 g·L^{-1} S/L, T = 373 K for 4 h and (B) stripping efficiency after DES contact with water at 1:1 mass ratio at room temperature for 1 h.

After the five leaching-stripping cycles, the DES integrity was verified by ^{1}H and ^{31}P NMR (**Figures S7** and **S8**) and Raman spectroscopy (**Figure S9**). The NMR and Raman spectra confirmed that the DES structure was not compromised after the five leaching-stripping cycles. Importantly, ^{1}H NMR results indicate that the initial molar fraction of the components in the original DES is maintained after five cycles. According to the ^{31}P NMR spectra, the P=O group environment after leaching is similar to that of the pristine DES. These results confirm that HCl is consumed throughout the leaching reaction and that the DES is not degraded during the leaching reaction. Altogether, the proposed leaching process has improved sustainability, demonstrating an alternative strategy to safely super concentrate HCl and quantitatively leach metals from spent cathodes. Complete leaching and simultaneous precipitation of Ni(II) are successfully accomplished under mild conditions, featuring low HCl concentrations. Furthermore, the process maintains its performance without being adversely affected by solvent regeneration, contributing to its sustainability. Compared to leaching with an equivalent aqueous HCl solution, the DES-HCl template has an enhanced efficiency and enables the simultaneous leaching and separation of Ni(II).

4. Conclusions

In this work, an atomically efficient process using DES as an HCl superconcentrator is proposed for the leaching and individual separation of the metallic fraction LIBs black mass material. The DES composed of TOPO:decanoic acid is shown to be able to super concentrate HCl 2.2-folds more than the conventional 37 wt% HCl in aqueous solution. At optimized conditions, the DES-loaded with 0.93 $mol \cdot L^{-1}$ HCl, 44 $g \cdot L^{-1}$ S/L, T = 373 K and t = 4 h can quantitatively leach Co(II), Mn(II) and Cu(II) from cathode powder whilst leaving 90% of Ni(II) in the solid residue as chloride salts. After leaching, the DES is easily regenerated by contacting it with water and the metal ions were simply separated using a two-step precipitation process. Approximately 98% of manganese was recovered as Mn_3O_4 with 81% purity after the addition of $KMnO_4$ and 99% of cobalt was subsequently recovered at 95% purity by precipitation with oxalic acid, leaving solely LiCl in solution. The proposed mild process removes the need for volatile organic solvents, and the DES could be successfully regenerated and reused for five cycles with no decrease in leaching efficiency or selectivity. As real waste BM material was used throughout, the process is resilient to the variability in BM composition and does not require the addition of an reducing agent, further reducing the chemical consumption. Nevertheless, a compromise between process simplicity and final product purity is apparent, particularly in the case of the Mn(II) product, with obtained purities being slightly lower than those obtained with other more complex approaches, such as solvent extraction. Additionally, further optimization is required to manage the deleterious influence of the DES viscosity after loading which affects both the yield of Ni(II) precipitation and solvent recovery. Even so, the reported system presents a better atom economy and enhanced sustainability compared to other DES and conventional inorganic acids, providing a new approach for the simultaneous leaching and separation of metals from LIBs. Future work is required to appreciate if the increased selectivity and atomic efficiency of the

proposed process is reflected in the environmental and economic impact of the process compared to traditional leaching media.

Table of abbreviations

$[M]_i$	**Metal concentration**
η	Dynamic viscosity
ρ	Density
A	frequency factor
AE	Atom economy
ChCl	Choline chloride
E^0	Electrode potential
E_a	Activation energy
EE%	Leaching extraction efficiency
ForA	Formic acid
HBTA	Benzoyltrifluoroacetone
k	Constant rate
LacA	Lactic acid
LCO	LiCoO2
NMC	$LiNi_xMn_yCo_zO_2$
NMR	Nuclear magnetic resonance spectroscopy
OxA	Oxalic acid
S%	Stripping extraction efficiency
SAXS	Small-angle X-ray scattering analysis
SCM	Shrinking core model
Sf	Separation factor
SHE	Standard hydrogen electrode
T_d	Decomposition temperature
TGA	Thermogravimetric analysis
TosA	p-toluenesulfonic acid
UV–Vis	Ultraviolet-visible
VFT	Vogel-Fulcher-Tammann

Acknowledgments

This work was developed within the scope of the project CICECO-Aveiro Institute of Materials, UIDB/50011/2020, UIDP/50011/2020 & LA/P/0006/2020, financed by national funds through the FCT/MEC (PIDDAC). Ana R. F. Carreira acknowledges FCT for the Ph.D. grant SFRH/BD/143612/2019. A.P.S. Crema acknowledges CAPES for the postdoctoral fellowship

(88887.474466/2020-00). Nicolas Schaeffer acknowledges the national funds (OE), through FCT–Fundação para a Ciência e a Tecnologia, I. P., in the scope of the framework contract foreseen in the numbers 4, 5, and 6 of the article 23, of the Decree-Law 57/2016, of August 29th, changed by Law 57/2017, of July 19th. Helena Passos acknowledges FCT – Fundação para a Ciência e a Tecnologia, I.P. for the researcher contract CEECIND/00831/2017 under the Scientific Employment Stimulus - Individual Call 2017. The authors thank Maria C.C. Azevedo and Márcia C. Neves for helping with Raman and SEM-EDS data acquisition, respectively.

Conflicts of interest: The authors declare no conflicts of interest.

References

[1] T. Kim, W. Song, D.Y. Son, L.K. Ono, Y. Qi, Lithium-ion batteries: outlook on present, future, and hybridized technologies, J Mater Chem A Mater. 7 (2019) 2942–2964. https://doi.org/10.1039/C8TA10513H.

[2] J. Pan, Z. Xia, N. Deng, L. Chen, H. Zhang, Y. Lu, Y. Liu, H. Gao, Eumelanin-inspired nanomaterials in electrochemical energy storage devices: A review, Chemical Engineering Journal. 452 (2023) 138607. https://doi.org/10.1016/j.cej.2022.138607.

[3] E. Pomerantseva, F. Bonaccorso, X. Feng, Y. Cui, Y. Gogotsi, Energy storage: The future enabled by nanomaterials, Science (1979). 366 (2019). https://doi.org/10.1126/science.aan8285.

[4] J.B. Goodenough, K.S. Park, The Li-ion rechargeable battery: A perspective, J Am Chem Soc. 135 (2013) 1167–1176. https://doi.org/10.1021/ja3091438.

[5] C.M. Costa, J.C. Barbosa, R. Gonçalves, H. Castro, F.J.D. Campo, S. Lanceros-Méndez, Recycling and environmental issues of lithium-ion batteries: Advances, challenges and opportunities, Energy Storage Mater. 37 (2021) 433–465. https://doi.org/10.1016/J.ENSM.2021.02.032.

[6] Race to Net Zero: The Pressures of the Battery Boom in Five Charts | BloombergNEF, (n.d.). https://about.bnef.com/blog/race-to-net-zero-the-pressures-of-the-battery-boom-in-five-charts/ (accessed March 9, 2023).

[7] European Commission, Critical Raw Materials Resilience: Charting a Path towards greater Security and Sustainability, (2020). https://eur-lex.europa.eu/legal-content/EN/TXT/PDF/?uri=CELEX:52020DC0474&from=EN (accessed April 18, 2023).

[8] T. Tawonezvi, M. Nomnqa, L. Petrik, B.J. Bladergroen, Recovery and Recycling of Valuable Metals from Spent Lithium-Ion Batteries: A Comprehensive Review and Analysis, Energies (Basel). 16 (2023) 1365. https://doi.org/10.3390/en16031365.

[9] L. Gaines, Lithium-ion battery recycling processes: Research towards a sustainable course, Sustainable Materials and Technologies. 17 (2018) e00068. https://doi.org/10.1016/J.SUSMAT.2018.E00068.

[10] X. Ma, M. Chen, Z. Zheng, D. Bullen, J. Wang, C. Harrison, E. Gratz, Y. Lin, Z. Yang, Y. Zhang, F. Wang, D. Robertson, S.B. Son, I. Bloom, J. Wen, M. Ge, X. Xiao, W.K. Lee, M. Tang, Q. Wang, J. Fu, Y. Zhang, B.C. Sousa, R. Arsenault, P. Karlson, N. Simon, Y. Wang, Recycled cathode materials enabled superior performance for lithium-ion batteries, Joule. 5 (2021) 2955–2970. https://doi.org/10.1016/j.joule.2021.09.005.

[11] European Commission, OECD Due Diligence Guidance for Responsible Supply Chains of Minerals from Conflict-Affected and High-Risk Areas, (2020). https://eur-lex.europa.eu/legal-content/EN/TXT/?uri=CELEX%3A52020PC0798 (accessed May 31, 2023).

[12] J. Neumann, M. Petranikova, M. Meeus, J.D. Gamarra, R. Younesi, M. Winter, S. Nowak, Recycling of Lithium-Ion Batteries—Current State of the Art, Circular Economy, and Next Generation Recycling, Adv Energy Mater. 12 (2022) 2102917. https://doi.org/10.1002/AENM.202102917.

[13] X. Wang, G. Gaustad, C.W. Babbitt, K. Richa, Economies of scale for future lithium-ion battery recycling infrastructure, Resour Conserv Recycl. 83 (2014) 53–62. https://doi.org/10.1016/J.RESCONREC.2013.11.009.

[14] G. Harper, R. Sommerville, E. Kendrick, L. Driscoll, P. Slater, R. Stolkin, A. Walton, P. Christensen, O. Heidrich, S. Lambert, A. Abbott, K. Ryder, L. Gaines, P. Anderson, Recycling lithium-ion batteries from electric vehicles, Nature. 575 (2019) 75–86. https://doi.org/10.1038/s41586-019-1682-5.

[15] J. Ju, Y. Feng, H. Li, C. Xu, Z. Xue, B. Wang, Extraction of valuable metals from minerals and industrial solid wastes via the ammonium sulfate roasting process: A systematic review, Chemical Engineering Journal. 457 (2023) 141197. https://doi.org/10.1016/j.cej.2022.141197.

[16] L.F. Zhou, D. Yang, T. Du, H. Gong, W. Bin Luo, The Current Process for the Recycling of Spent Lithium Ion Batteries, Front Chem. 8 (2020) 1027. https://doi.org/10.3389/fchem.2020.578044.

[17] P. Moazzam, Y. Boroumand, P. Rabiei, S.S. Baghbaderani, P. Mokarian, F. Mohagheghian, L.J. Mohammed, A. Razmjou, Lithium bioleaching: An emerging approach for the recovery of Li from spent lithium ion batteries, Chemosphere. 277 (2021) 130196. https://doi.org/10.1016/j.chemosphere.2021.130196.

[18] R.E. Ciez, J.F. Whitacre, Examining different recycling processes for lithium-ion batteries, Nat Sustain. 2 (2019) 148–156. https://doi.org/10.1038/s41893-019-0222-5.

[19] Y. Li, W. Lv, H. Huang, W. Yan, X. Li, P. Ning, H. Cao, Z. Sun, Recycling of spent lithium-ion batteries in view of green chemistry, Green Chemistry. 23 (2021) 6139–6171. https://doi.org/10.1039/D1GC01639C.

[20] Ankit, L. Saha, V. Kumar, J. Tiwari, Sweta, S. Rawat, J. Singh, K. Bauddh, Electronic waste and their leachates impact on human health and environment: Global ecological threat and management, Environ Technol Innov. 24 (2021) 102049. https://doi.org/10.1016/J.ETI.2021.102049.

[21] E.M. Iannicelli-Zubiani, M.I. Giani, F. Recanati, G. Dotelli, S. Puricelli, C. Cristiani, Environmental impacts of a hydrometallurgical process for electronic waste treatment: A life cycle assessment case study, J Clean Prod. 140 (2017) 1204–1216. https://doi.org/10.1016/J.JCLEPRO.2016.10.040.

[22] L. Rocchetti, F. Vegliò, B. Kopacek, F. Beolchini, Environmental impact assessment of hydrometallurgical processes for metal recovery from WEEE residues using a portable prototype plant, Environ Sci Technol. 47 (2013) 1581–1588. https://doi.org/10.1021/es302192t.

[23] Y. Pranolo, W. Zhang, C.Y. Cheng, Recovery of metals from spent lithium-ion battery leach solutions with a mixed solvent extractant system, Hydrometallurgy. 102 (2010) 37–42. https://doi.org/10.1016/J.HYDROMET.2010.01.007.

[24] H. Guo, G. Kuang, H. Wan, Y. Yang, H. zhao Yu, H. dong Wang, Enhanced acid treatment to extract lithium from lepidolite with a fluorine-based chemical method, Hydrometallurgy. 183 (2019) 9–19. https://doi.org/10.1016/J.HYDROMET.2018.10.020.

[25] M.K. Jha, A. Kumari, A.K. Jha, V. Kumar, J. Hait, B.D. Pandey, Recovery of lithium and cobalt from waste lithium ion batteries of mobile phone, Waste Management. 33 (2013) 1890–1897. https://doi.org/10.1016/J.WASMAN.2013.05.008.

[26] H. Bastos, N. Schaeffer, J.M. Pringle, J.A.P. Coutinho, C. Pozo-Gonzalo, Enhanced Dissolution of Metal Oxides in Hydroxylated Solvents – Towards Application in Lithium-Ion Battery Leaching, ChemSusChem. (2023) e202300455. https://doi.org/10.1002/CSSC.202300455.

[27] K. Huang, H. Zhou, A. He, Y. Sun, Y. Liu, X. Gao, Y. Zhao, S. Liu, Z. Li, T. Hu, X. Li, C. Liu, Y. Wei, L. Yang, J. Feng, Y. Cai, Z. Yang, Y. Xu, I. Noda, J. Wu, Superconcentrated hydrochloric acid, Journal of Physical Chemistry B. 115 (2011) 7823–7829. https://doi.org/10.1021/jp109551z.

[28] R. Guo, L. Guo, K. Huang, A. He, J. Zhang, L. Zheng, Y. Liu, T. Kang, X. Gao, S. Weng, Y. Zhao, Z. Yang, Y. Xu, I. Noda, J. Wu, Investigation on the trioctylphosphine oxide-based super-concentrated HCl system, Spectrochim Acta A Mol Biomol Spectrosc. 136 (2015) 288–294. https://doi.org/10.1016/j.saa.2014.08.133.

[29] X. Li, K. Binnemans, Oxidative Dissolution of Metals in Organic Solvents, Chem Rev. 121 (2021) 4506–4530. https://doi.org/10.1021/acs.chemrev.0c00917.

[30] T. Palden, M. Regadío, B. Onghena, K. Binnemans, Selective Metal Recovery from Jarosite Residue by Leaching with Acid-Equilibrated Ionic Liquids and Precipitation-Stripping, ACS Sustain Chem Eng. 7 (2019) 4239–4246. https://doi.org/10.1021/acssuschemeng.8b05938.

[31] V.N.H. Nguyen, S.J. Song, M.S. Lee, Separation of palladium and platinum metals by selective and simultaneous leaching and extraction with aqueous/non-aqueous solutions, Hydrometallurgy. 208 (2022) 105814. https://doi.org/10.1016/J.HYDROMET.2021.105814.

[32] R. Chiarizia, D. Stepinski, M.R. Antonio, Sans study of HCl extraction by selected neutral organophosphorus compounds in n-octane, Sep Sci Technol. 45 (2010) 1668–1678. https://doi.org/10.1080/01496395.2010.493828.

[33] D.O. Abranches, J.A.P. Coutinho, Everything You Wanted to Know about Deep Eutectic Solvents but Were Afraid to Be Told, Annu Rev Chem Biomol Eng. 14 (2023) 141–163. https://doi.org/10.1146/annurev-chembioeng-101121-085323.

[34] N. Schaeffer, J.H.F. Conceição, M.A.R. Martins, M.C. Neves, G. Pérez-Sánchez, J.R.B. Gomes, N. Papaiconomou, J.A.P. Coutinho, Non-ionic hydrophobic eutectics – versatile solvents for tailored metal separation and valorisation, Green Chemistry. 22 (2020) 2810–2820. https://doi.org/10.1039/d0gc00793e.

[35] R. Lommelen, T. Vander Hoogerstraete, B. Onghena, I. Billard, K. Binnemans, Model for Metal Extraction from Chloride Media with Basic Extractants: A Coordination Chemistry Approach, Inorg Chem. 58 (2019) 12289–12301. https://doi.org/10.1021/acs.inorgchem.9b01782.

[36] Y. Tian, B. Etschmann, W. Liu, S. Borg, Y. Mei, D. Testemale, B. O'Neill, N. Rae, D.M. Sherman, Y. Ngothai, B. Johannessen, C. Glover, J. Brugger, Speciation of nickel (II) chloride complexes in hydrothermal fluids: In situ XAS study, Chem Geol. 334 (2012) 345–363. https://doi.org/10.1016/j.chemgeo.2012.10.010.

[37] W.S. Chen, H.J. Ho, Recovery of Valuable Metals from Lithium-Ion Batteries NMC Cathode Waste Materials by Hydrometallurgical Methods, Metals (Basel). 8 (2018) 321. https://doi.org/10.3390/MET8050321.

[38] W. Xuan, nio de Souza Braga, A. Chagnes, Development of a Novel Solvent Extraction Process to Recover Cobalt, Nickel, Manganese, and Lithium from Cathodic Materials of Spent Lithium-Ion Batteries, 16 (2023) 40. https://doi.org/10.1021/acssuschemeng.1c07109.

[39] A. Chernyaev, J. Partinen, L. Klemettinen, B.P. Wilson, A. Jokilaakso, M. Lundström, The efficiency of scrap Cu and Al current collector materials as reductants in LIB waste leaching, Hydrometallurgy. 203 (2021) 105608. https://doi.org/10.1016/j.hydromet.2021.105608.

[40] S.J.R. Vargas, G. Pérez-Sánchez, N. Schaeffer, J.A.P. Coutinho, Solvent extraction in extended hydrogen bonded fluids - separation of Pt(iv) from Pd(ii) using TOPO-based type V DES, Green Chemistry. 23 (2021) 4540–4550. https://doi.org/10.1039/d1gc00829c.

[41] U.G. Favero, N. Schaeffer, H. Passos, K. A. M. L. Cruz, D. Ananias, S. Dourdain, M.C. Hespanhol, Solvent extraction in non-ideal eutectic solvents – Application towards lanthanide separation, Sep Purif Technol. 314 (2023) 123592. https://doi.org/10.1016/J.SEPPUR.2023.123592.

[42] M. Taherzadeh, R. Haghbakhsh, A.R.C. Duarte, S. Raeissi, Estimation of the heat capacities of deep eutectic solvents, J Mol Liq. 307 (2020) 112940. https://doi.org/10.1016/J.MOLLIQ.2020.112940.

[43] R.C.F. Schaake, J.C. van Miltenburg, C.G. de Kruif, Thermodynamic properties of the normal alkanoic acids II. Molar heat capacities of seven even-numbered normal alkanoic acids, J Chem Thermodyn. 14 (1982) 771–778. https://doi.org/10.1016/0021-9614(82)90173-2.

[44] J. Hulnink, K. van Miltenburg, H.A.J. Oonk, A. Schuljff, P. Groen, Thermodynamic Functions and Vapor Pressures of Triphenylphosphine Oxide and 1,4-Bis(diphenylphosphino)butane Near the Melting Point, J Chem Eng Data. 34 (1989) 99–100. https://doi.org/10.1021/je00055a028.

[45] J.M. Hogg, L.C. Brown, K. Matuszek, P. Latos, A. Chrobok, M. Swadźba-Kwaśny, Liquid coordination complexes of Lewis acidic metal chlorides: Lewis acidity and insights into speciation, Dalton Transactions. 46 (2017) 11561–11574. https://doi.org/10.1039/C7DT02408H.

[46] E. Billy, M. Joulié, R. Laucournet, A. Boulineau, E. De Vito, D. Meyer, Dissolution Mechanisms of LiNi1/3Mn1/3Co1/3O2 Positive Electrode Material from Lithium-Ion Batteries in Acid Solution, ACS Appl Mater Interfaces. 10 (2018) 16424–16435. https://doi.org/10.1021/acsami.8b01352.

[47] W. Xuan, A. de Souza Braga, C. Korbel, A. Chagnes, New insights in the leaching kinetics of cathodic materials in acidic chloride media for lithium-ion battery recycling, Hydrometallurgy. 204 (2021) 105705. https://doi.org/10.1016/J.HYDROMET.2021.105705.

[48] Y. Marcus, Metal-chloride complexes studied by ion-exchange and solvent-extraction methods. PartI. Non-transition-metalions, lanthanides, actinides, and d° transition-metal ions, Coord Chem Rev. 2 (1967) 195–238. https://doi.org/10.1016/s0010-8545(00)80205-2.

[49] E. Hogfeldt, Stability constants of metal-ion complexes. Part A, Inorganic ligands, Pergamon Press, Oxford, 1982.

[50] M. Gras, N. Papaiconomou, N. Schaeffer, E. Chainet, F. Tedjar, J.A.P. Coutinho, I. Billard, Ionic-Liquid-Based Acidic Aqueous Biphasic Systems for Simultaneous Leaching and Extraction of Metallic Ions, Angewandte Chemie. 130 (2018) 1579–1582. https://doi.org/10.1002/ange.201711068.

[51] X. Chang, M. Fan, C.F. Gu, W.H. He, Q. Meng, L.J. Wan, Y.G. Guo, Selective Extraction of Transition Metals from Spent LiNixCoyMn1−x−yO2 Cathode via Regulation of Coordination Environment, Angewandte Chemie International Edition. 61 (2022) e202202558. https://doi.org/10.1002/ANIE.202202558.

[52] M.L. Free, Hydrometallurgy: Fundamentals and applications, Hydrometallurgy: Fundamentals and Applications. (2014) 1–432. https://doi.org/10.1002/9781118732465.

[53] A.F. Yi, Z.W. Zhu, Y.H. Liu, J. Zhang, H. Su, T. Qi, Using highly concentrated chloride solutions to leach valuable metals from cathode-active materials in spent lithium-ion batteries, Rare Metals. 40 (2021) 1971–1978. https://doi.org/10.1007/s12598-020-01503-4.

[54] A. Chernyaev, Y. Zou, B.P. Wilson, M. Lundström, The interference of copper, iron and aluminum with hydrogen peroxide and its effects on reductive leaching of LiNi1/3Mn1/3Co1/3O2, Sep Purif Technol. 281 (2022) 119903. https://doi.org/10.1016/J.SEPPUR.2021.119903.

[55] K.S. Yamaguchi, D.T. Sawyer, The Redox Chemistry of Manganese(III) and -(IV) Complexes, Isr J Chem. 25 (1985) 164–176. https://doi.org/10.1002/IJCH.198500026.

[56] M. Joulié, E. Billy, R. Laucournet, D. Meyer, Current collectors as reducing agent to dissolve active materials of positive electrodes from Li-ion battery wastes, Hydrometallurgy. 169 (2017) 426–432. https://doi.org/10.1016/J.HYDROMET.2017.02.010.

[57] P. Meshram, B.D. Pandey, T.R. Mankhand, Recovery of valuable metals from cathodic active material of spent lithium ion batteries: Leaching and kinetic aspects, Waste Management. 45 (2015) 306–313. https://doi.org/10.1016/j.wasman.2015.05.027.

[58] P. Meshram, B.D. Pandey, T.R. Mankhand, Hydrometallurgical processing of spent lithium ion batteries (LIBs) in the presence of a reducing agent with emphasis on kinetics of leaching, Chemical Engineering Journal. 281 (2015) 418–427. https://doi.org/10.1016/j.cej.2015.06.071.

[59] C.K. Lee, K.I. Rhee, Reductive leaching of cathodic active materials from lithium ion battery wastes, Hydrometallurgy. 68 (2003) 5–10. https://doi.org/10.1016/S0304-386X(02)00167-6.

[60] X. Zheng, W. Gao, X. Zhang, M. He, X. Lin, H. Cao, Y. Zhang, Z. Sun, Spent lithium-ion battery recycling – Reductive ammonia leaching of metals from cathode scrap by sodium sulphite, Waste Management. 60 (2017) 680–688. https://doi.org/10.1016/j.wasman.2016.12.007.

[61] R. Golmohammadzadeh, F. Rashchi, E. Vahidi, Recovery of lithium and cobalt from spent lithium-ion batteries using organic acids: Process optimization and kinetic aspects, Waste Management. 64 (2017) 244–254. https://doi.org/10.1016/j.wasman.2017.03.037.

[62] J. Li, P. Shi, Z. Wang, Y. Chen, C.C. Chang, A combined recovery process of metals in spent lithium-ion batteries, Chemosphere. 77 (2009) 1132–1136. https://doi.org/10.1016/J.CHEMOSPHERE.2009.08.040.

[63] M. Joulié, R. Laucournet, E. Billy, Hydrometallurgical process for the recovery of high value metals from spent lithium nickel cobalt aluminum oxide based lithium-ion batteries, J Power Sources. 247 (2014) 551–555. https://doi.org/10.1016/J.JPOWSOUR.2013.08.128.

[64] S.P. Barik, G. Prabaharan, L. Kumar, Leaching and separation of Co and Mn from electrode materials of spent lithium-ion batteries using hydrochloric acid: Laboratory and pilot scale study, J Clean Prod. 147 (2017) 37–43. https://doi.org/10.1016/J.JCLEPRO.2017.01.095.

[65] N. Peeters, K. Janssens, D. de Vos, K. Binnemans, S. Riaño, Choline chloride–ethylene glycol based deep-eutectic solvents as lixiviants for cobalt recovery from lithium-ion battery cathode materials: are these solvents really green in high-temperature processes?, Green Chemistry. 24 (2022) 6685–6695. https://doi.org/10.1039/D2GC02075K.

[66] T.T. Tran, H.S. Moon, M.S. Lee, Recovery of valuable metals from the hydrochloric leaching solution of reduction smelted metallic alloys from spent lithium-ion batteries, Journal of Chemical Technology and Biotechnology. 97 (2022) 1247–1258. https://doi.org/10.1002/jctb.7019.

[67] Q. Lu, L. Chen, X. Li, Y. Chao, J. Sun, H. Ji, W. Zhu, Sustainable and Convenient Recovery of Valuable Metals from Spent Li-Ion Batteries by a One-Pot Extraction Process, ACS Sustain Chem Eng. 9 (2021) 13851–13861. https://doi.org/10.1021/acssuschemeng.1c04717.

[68] R. Morina, D. Callegari, D. Merli, G. Alberti, P. Mustarelli, E. Quartarone, Cathode Active Material Recycling from Spent Lithium Batteries: A Green (Circular) Approach Based on Deep Eutectic Solvents, ChemSusChem. 15 (2022) e202102080. https://doi.org/10.1002/cssc.202102080.

[69] L. Chen, Y. Chao, X. Li, G. Zhou, Q. Lu, M. Hua, H. Li, X. Ni, P. Wu, W. Zhu, Engineering a tandem leaching system for the highly selective recycling of valuable metals from spent Li-ion batteries, Green Chemistry. 23 (2021) 2177–2184. https://doi.org/10.1039/d0gc03820b.

[70] T. Hanada, M. Goto, Cathode recycling of lithium-ion batteries based on reusable hydrophobic eutectic solvents, Green Chemistry. 24 (2022) 5107–5115. https://doi.org/10.1039/d1gc04846e.

[71] T. Hanada, M. Goto, Synergistic Deep Eutectic Solvents for Lithium Extraction, ACS Sustain Chem Eng. 9 (2021) 2152–2160. https://doi.org/10.1021/ACSSUSCHEMENG.0C07606.

Highlights

- DES-loaded with HCl is a suitable medium for leaching spent LIB.
- 90% of Ni(II) was selectively precipitated during leaching.
- Co(II), Mn(II) and Cu(II) were quantitatively leached.
- The designed leaching is selective and has good atom economy (89%).
- 99% of Co(II) was easily precipitated and recovered with a purity of 95%.